Adaptive fuzzy PID integrated renewable power management system for off grid and on grid conditions

Veeranjaneyulu Gopu[1], Mudakapla Shadaksharappa Nagaraj[2]
[1]Department of Electrical and Electronics Engineering, Visvesvaraya Technological University, Belagavi, India
[2]Department of Electrical and Electronics Engineering, Bapuji Institute of Engineering and Technology, Davangere, India

Article Info

ABSTRACT

Renewable source penetration into the distribution grid is merely a greater challenge as the powers from renewable sources are not stable and constant. Due to their sporadic operating states the power shared to the grid creates power quality issues. Therefore, an efficient adaptive PMA needs to be adopted for the control of these renewable sources, which controls the power extraction of these sources. For standard power sharing to the variable loads in the grid islanding state, the renewable sources are updated with the ESS module. In this paper, a low-rating distribution test system is considered connected with different renewable sources PV sources, wind farms, and fuel cell plants sharing renewable power. The PV source module is updated with AF-PID replacing the PI controller integrated PMA and ESS module for extensive control of the power of the generation unit during any operating condition. The DC and AC voltages are more stabilized by the upgraded PMA during grid islanding conditions. Mitigation of ripple and harmonic content is achieved by the AF-PID controller varying the proportional, integral, and derivative gains as per the error signal generated. A comparative analysis is carried out on the system validating the effectiveness of the AF-PID controller using MATLAB Simulink software.

Corresponding Author:

Veeranjaneyulu Gopu
Department of Electrical and Electronics Engineering, Visvesvaraya Technological University
Belagavi-590018, India
Email: gvanjaneyulu@rvrjc.ac.in, gvvtu2023@mail.com

1. INTRODUCTION

In today's power grid system, there is an emphasis on renewable energy penetration with bulk power generation meeting the load demands replacing conventional power generation to mitigate carbon print in the environment. There are many options for renewable power generation which majorly include PV sources, wind farms, fuel cell plants, biogas plants, and tidal energy systems. These renewable sources are majorly located at farther distances from the main grid to avoid human intervention and the availability of natural resources. From the mentioned renewable sources, the PV source is considered to be the best choice because of its low maintenance, lower economy, and consistence [1]. The next choices would be wind farms and fuel cell plants which are also a huge contribution to the renewable grid. For our analysis, a simple distribution grid is considered with multiple buses, loads, and transmission lines integrated with these renewable power sources at different bus locations [2]. These sources share power to the grid in parallel with the conventional source in synchronization supporting the local loads.

In previous research, the renewable sources connected to the grid are disconnected when the grid is isolated to avoid dependency on renewable sources. For this an islanding detection algorithm is included at the renewable source modules which triggers the breaker off, disconnecting the sources from the main grid. Due

to this disconnection, there is reliability issue in the system [3]. During grid islanding condition the critical and essential loads are not compensated which needs necessary power. Therefore, a local backup storage power needs to be provided for the essential load to get compensated during grid islanding conditions.

Each renewable source unit (PV source, wind farm, and fuel cell plant) has its power converters and individual controllers for stable voltage generation. The controllers take feedback from the local bus for synchronizing the renewable unit to the grid voltages. From the given renewable source units, the PV source is updated with ESS support for sharing power during grid islanding conditions. This study compares the performance of a PV module integrated with an ESS unit (which consists of a battery and supercapacitor) against the standalone operation of a wind farm and a fuel cell plant. The research introduces a PMA that controls the power exchange of the ESS unit. During grid isolation conditions, the PV module and ESS unit are operated in standalone mode, providing support to the local essential load. According to previous study [4], a conventional PI controller is used to operate the converters of the sources in the hybrid AC/DC microgrid, but it has high damping and disturbances that create harmonics in the voltages. The research suggests replacing the PI controller with an AF-PI controller in the PMA, which operates at lower damping and creates smoother reference signals [4]. The outline design of the proposed distribution grid with renewable source units can be seen in Figure 1.

In the given distribution system Figure 1 the feeder bus is connected to the main utility source, feeding power at 132 kV. The 132 kV voltage is stepped down to distribution voltage at 11 kV feeding the buses 1-4. Each bus is integrated with multiple loads connected through 11 kV/440 V distribution transformers. The renewable source units are connected at buses 1, 3, and 4 as the local load demand is higher. The bus 1 is integrated with a PV source and ESS unit, bus 3 with the wind farm, and bus 4 with a fuel cell plant. The PMA is applied to the renewable source module which has ESS integrated [5].

The ESS comprises of battery pack and supercapacitor (SC) operated through a bidirectional DC-DC converter (BDC) [6]. The switches of these BDCs are controlled by the PMA as per the PV source power and load demand on bus 1. An islanding detection algorithm is included for tripping ESS unit ON during grid isolation conditions supporting the essential load. During the grid isolation condition all the other breakers are tripped OFF disconnecting other loads from the feeder line [7], [8]. Only the PV source with ESS unit will be operated supporting the local essential load (L1-2) managed by PMA.

The paper is arranged with the introduction in section 1 followed by the renewable source unit's configuration in section 2. The section 3 is included with PMA design with AF-PID control structure modeling. The simulation results and analysis are done in section 4 followed by a conclusion to the paper in section 5. At the end, the reference papers are provided that are cited in this paper.
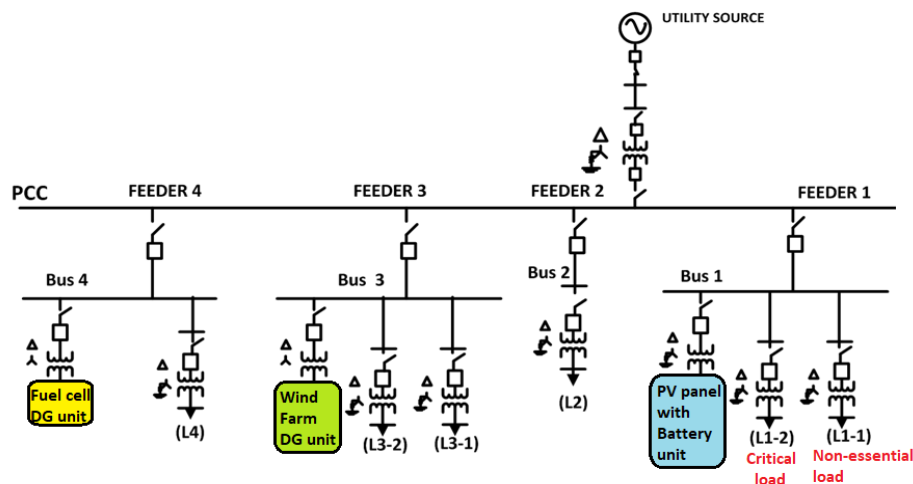

Figure 1. Proposed distribution grid with renewable source units

2. METHOD

2.1. Renewable sources and PMA

As mentioned previously the priority renewable sources are considered to be PV source, wind farm and fuel cell interconnected at the buses 1, 3, and 4 respectively. All the renewable sources generate unstable power as per the availability of natural sources like solar radiation, wind speed, hydrogen gas. The voltages from these sources need to be stabilized by power converters with individual control structures. The control structures operate with feedback from the sources and the interconnected grid bus.

The PV source is combination of multiple similar rating PV panels from a single manufacturer connected in parallel and series strings. The number of series panels that needs to be connected to form a string is decided by the voltage amplitude required to inject power to the grid. These PV panels are integrated with DC-DC quadratic boost converter (QBC) operated using perturb and observe (P&O) MPPT algorithm for maximum power extraction from the panels with respect to solar radiation [9]. The QBC is connected to a 3-ph inverter for converting the DC voltage to 3-ph AC voltages operated by synchronous reference frame (SRF) control with feedback from interconnected bus 1.

The wind farm renewable unit is adopted with PMSG machine which is an independent generator without any external excitation or grid feeding. The PMSG is driven by wind turbine with mechanical torque input generated as per the blades pitch angle and wind speed [10]. The PMSG is connected to a rectifier converting unstable AC voltage to DC voltage. The DC voltage is further refined to stable DC with unidirectional buck-boost DC-DC converter operated by power signal feedback (PSF) MPPT control structure [11]. The maximum power extracted from PMSG is converter to 3-ph AC by the inverter operated by same SRF controller operating in synchronization to the interconnected bus 3. The fuel cell plant is similar to PV source unit comprising of conventional boost converter for boosting the voltage of fuel cell to required amplitude. However, the boost converter is operated by constant voltage (CV) feedback control with specific reference voltage feedback [12]. The boost converter further connected with inverter for AC voltage generation operated by the same SRF control for synchronization to the bus 4.

These renewable sources are designed to be operated only during grid availability. When the conventional utility grid source is isolated from the distribution grid due to faults on the lines or source side these renewable sources cannot be operated in standalone mode [13]. In order to operate these sources in standalone condition during grid source isolation an ESS unit need to be installed in parallel to these sources at the DC link. The ESS unit supports the renewable source by stabilizing the voltage at the bus with independent controllers [14]. The ESS unit supports the sources either by storing excess power or by providing deficit power to the loads with respect to unpredictable renewable power generated. For our analysis the ESS unit is included into the PV source module support the local essential load on bus 1. The ESS unit comprises of a battery pack and SC unit connected to the PV source QBC through BDCs [15]. The internal circuit structure of the PV source module can be observed in Figure 2 with batter pack and SC.

As observed in Figure 2 each individual circuit topology comprises of controllable power electronic switches which need to be operated as per the requirement of the system [16]. The QBC switch S is controlled by P&O MPPT algorithm as mentioned previously taking feedback from PV array voltage and current. The BDC circuit switches of both the modules (battery and SC) are controlled by a PMA which controls the charging and discharging of these storage units [17]. The Figure 3 is the adopted PMA for the above storage units.

In the given control structure, the storage modules are controlled by current reference generation using the PMA [18]. The PMA generates i*scr (SC current) and i*Br (battery current) with respect to current required for the system to maintain the DC link voltage at specific value. Table 1 shows the current outputs for the given state of charge (SOC) of the battery and SC [13]. In Table 1, the reference currents of the battery or SC are given 0, when the SOC_b or SOC_{sc} are either above upper limit (U = 95%) or below lower limit (L = 10%) [14]. During insufficient power mode, the battery current is determined with integral multiple value λ which is given in Table 2.

Table 1. PMA current reference table

	SOC range	Reference currents
Insufficient power mode	SOCb > L ; SOCsc > L	$i_{Br}^* = \lambda i_t^*$; $i_{scr}^* = i_t'$
	SOCb < L ; SOCsc > L	$i_{Br}^* = 0$; $i_{scr}^* = i_t'$
	SOCb > L ; SOCsc < L	$i_{Br}^* = \lambda i_t^*$; $i_{scr}^* = 0$
	SOCb < L ; SOCsc < L	$i_{Br}^* = 0$; $i_{scr}^* = 0$
Sufficient and floating power mode	SOCb < U ; SOCsc < U	$i_{Br}^* = i_{B.ch}$; $i_{scr}^* = i_{SC.ch}$
	SOCb < U ; SOCsc > U	$i_{Br}^* = i_{B.ch}$; $i_{scr}^* = i_t'$
	SOCb > U ; SOCsc < U	$i_{Br}^* = 0$; $i_{scr}^* = i_{SC.ch}$
	SOCb > U ; SOCsc > U	$i_{Br}^* = 0$; $i_{scr}^* = i_t'$

Table 2. λ selection table

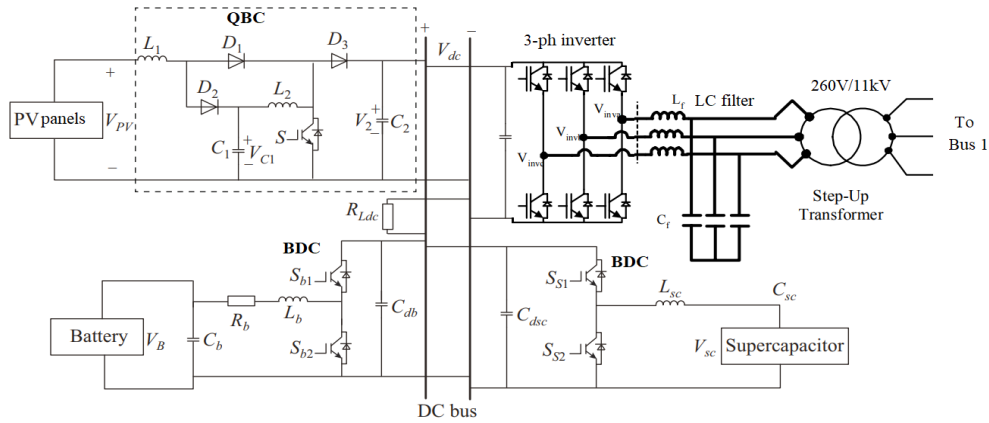| SOCb	λ
0.8 < SOCb < 0.95	1
0.45 < SOCb < 0.8	0.6
0.15 < SOCb < 0.45	0.3
SOCb < 0.15	0

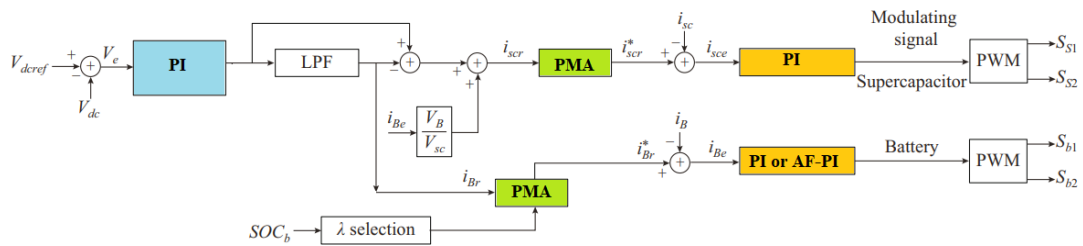Figure 2. The internal circuit structure of the PV source with ESS unit at bus 1

Figure 3. The control structure of storage modules with PMA

The operative current (i_t^*), transient operative current (i_t'), battery charging current ($i_{B.ch}$) and SC charging current ($i_{SC.ch}$) calculations are expressed as (1)-(4).

$$i_t^* = \frac{w_c}{s+w_c} i_t \tag{1}$$

$$i_t' = \left(1 - \frac{w_c}{s+w_c}\right) i_t \tag{2}$$

$$i_{B.ch} = \frac{-P_{Br}}{V_B} \tag{3}$$

$$i_{SC.ch} = -P_{sc}\sqrt{\frac{C_{sc}}{2E_{sc}}} \tag{4}$$

In (1)-(4), 'w_c' is the angular cut off frequency set at $2\pi.10$ considering 10 Hz as the cut off frequency. 'P_{Br}' is the battery power and 'V_B' is the battery voltage. 'P_{sc}', 'C_{sc}' and 'E_{sc}' are the SC power, SC capacity and SC energy respectively. In both the charging currents expression of the battery and SC the negative symbol represents charging [14]. The current 'i_t' is expressed as (5).

$$i_t = \left(V_{dc\,ref} - V_{dc}\right)(K_p + \int K_i) \tag{5}$$

Here, 'K_p' and 'K_i' are the DC voltage controller proportional and integral gains set by tuning the values as per the response of the system and settling of the DC link voltage. After the reference currents i_{Br}^* and i_{scr}^* generation they are compared to measured battery and SC currents (ib and isc) and the error is fed to current controllers generating duty ratio of the switches Sb1, Sb2, Sc1 and Sc2. The switches Sb1 and Sb2 of battery module, Sc1 and Sc2 of SC module are complimentary operating switches with NOT gate connected [14]. The current controller of the SC is PI controller and the battery current controller is updated with AF-PID for better DC link voltage regulation improving peak overshoot and ripple in the voltage [19].

2.2. AF-PID controller design

　　　　The adaptive fuzzy–PID (AF-PID) controller is considered to be an advanced control module for the PMA. The conventional PI controller in the PMA has more disturbances and has higher damping for the error input given. Due to higher damping, the peak overshoots are high, a ripple in the voltage is high, and the settling time is also high. This creates more disturbances at the DC link voltage of the system inducing the same into the AC side creating power quality issues. The AF-PID design varies the gains Kp, Ki, and Kd (proportional, integral, and derivative) gain of the conventional PID controller with respect to the error input given by comparing the reference values with actual values [20]. Figure 4 is the design of the AF-PID controller with variable gains of the PID controller.

　　　　As seen in Figure 4 there are two inputs to the fuzzy controller noted as error (e) and change in error (Δe) generated using derivative block. The Δe is the value generated by comparison of present value of error 'e(k)' with the previous value of error 'e(k-1)' [21]. The output of the fuzzy controller has three variables (Kp1, Ki1, and Kd1) which are gains of the conventional PID controller. The input variables (e and Δe) are set with seven triangular shape membership functions with the range given as per the maximum and minimum limits of the input variables. Figure 5 is the membership functions design of the input variables 'e' and 'Δe' [22]. As per the above design the input variable 'e' is given a range from -100 to 100 and the variable 'Δe' is given the range of -1 to 1. The output variable can be any of the gains of the PID controller which is also designed with seven gauss type membership functions as shown in Figure 6 [20].
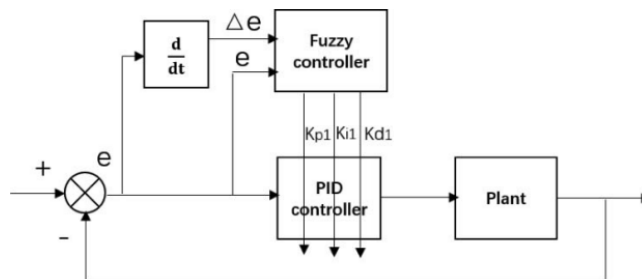

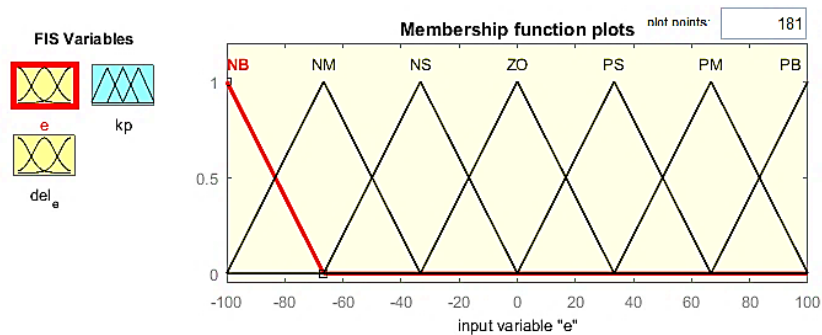Figure 4. AF-PID internal control structure

Figure 5. Input variables 'e' and 'Δe' seven membership functions design
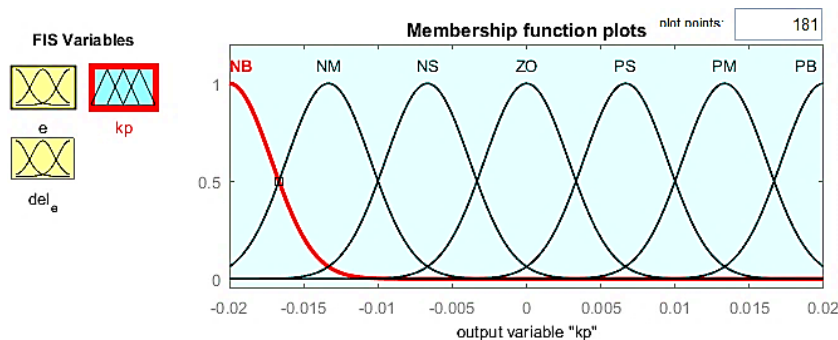

Figure 6. Output variable 'Kp1' membership functions design

The range of the output variable 'Kp' is set between -0.02 to 0.02 tuned as per the response of the controller to the changes that occurred in the test system. Each membership function is named as per the region it is in, given as negative big (NB), negative medium (NM), negative small (NS), zero (ZO), positive small (PS), positive medium (PM) and positive big (PB) [23]. These membership functions are set with balanced equal space between them covering the complete range of the output variable. The other two output variables 'Ki1' and 'Kd1' are also designed with the same seven membership functions and names but with a change in the range of the variables. These membership functions of the variables (e, Δe, Kp1 Ki1, and Kd1) are mapped with a fuzzy rule base (fuzzy fiction) of 49 rules for each output variable given in Tables 3-5 [20].

Table 3. Rule base for Kp1 gain variable

49 rule base		Error signal (e)						
		NB	NM	NS	ZO	PS	PM	PB
	NB	PB	PB	PM	PM	PS	ZO	ZO
	NM	PB	PB	PM	PS	PS	ZO	NS
	NS	PM	PM	PM	PS	ZO	NS	NS
Change in error (Δe)	ZO	PM	PM	PS	ZO	NS	NM	NM
	PS	PS	PS	ZP	NS	NS	NM	NM
	PM	PS	ZO	NS	NM	NM	NM	NB
	PB	ZO	ZO	NM	NM	NM	NB	NB

Table 4. Rule base for Ki1 gain variable

49 rule base		Error signal (e)						
		NB	NM	NS	ZO	PS	PM	PB
	NB	NB	NB	NM	NM	NS	ZO	ZO
	NM	NB	NB	NM	NS	NS	ZO	ZO
	NS	NB	NM	NS	NS	ZO	PS	PS
Change in error (Δe)	ZO	NM	NM	NS	ZO	PS	PM	PM
	PS	NM	NS	ZO	PS	PS	PM	PM
	PM	ZO	ZO	PS	PS	PM	PM	PB
	PB	ZO	ZO	PS	PM	PM	PB	PB

Table 5. Rule base for Kd1 gain variable

49 rule base		Error signal (e)						
		NB	NM	NS	ZO	PS	PM	PB
	NB	PS	NS	NB	NB	NB	NM	ZO
	NM	PS	NS	NB	NM	NM	NS	ZO
	NS	ZO	NS	NS	NM	NS	NS	ZO
Change in error (Δe)	ZO	ZO	NS	NS	NS	NS	NS	ZO
	PS	ZO	ZO	ZO	ZO	ZO	ZO	ZO
	PM	PM	NS	PS	PS	PM	PM	PB
	PB	PB	PM	PM	PM	PS	PS	PB

As per Tables 3-5 given the rule base of the output variables Kp1, Ki1, and Kd1 gains the values are updated to the conventional PID controller [24]. The dynamic response of the PID controller to the error value generated at the input will improve the battery module BDC operation response time [23]. As per the duty ratio generated by the AF-PID controller, the DC link voltage is stabilized with lower ripple, peak overshoots, and higher amplitude. This creates better compensation for the essential load during grid isolation conditions [25].

3. RESULTS AND ANALYSIS

The given test system with feeder lines connected to grid feeding multiple loads at bus 1, 2, 3, and 4 is modeled integrating PV source, Wind farm and fuel cell plant at buses 1, 3, and 4 respectively. The PV source is updated with ESS operated with PMA supporting the PV source in grid isolation condition. The PMA is later on updated with AF-PID controller in the battery control replacing conventional PI controller and comparative analysis is done with both the controllers in the PMA. Table 6 are the parameters considered for the modeling of the test system with renewable source units, ESS, and PMA modules.

As per the given configuration parameters the test system is run with different operating conditions validating the performance of ESS and PMA. Initially, the grid is connected to the feeder lines compensating loads sharing power with renewable sources. The complete simulation time considered is 3 sec in which the grid is connected from 0-1 sec. At 1 sec the grid is isolated from the feeder lines disconnecting the wind farm and fuel cell plant from the grid, activating the ESS and PMA modules in the PV source unit. The non-essential loads are disconnected from bus 1 and also disconnecting bus 1 from the main feeder system by the islanding

detection algorithm. At 2 sec the solar irradiation is dropped to half where the ESS supports the essential loads maintaining the voltage at the rated value. Figure 7 shows the graphs generated for the given operating conditions of the test system with different parameters plotted with respect to time.

Figures 7(a)-7(b) show the graphs of the grid voltage in per-unit and active, reactive powers of the main grid source. All the graphs are dropped to '0' at 1sec as the grid is isolated by a circuit breaker creating grid islanding conditions. During grid isolation conditions the wind farm and the fuel cell plant are disconnected from the distribution grid to avoid damage to the renewable sources. Along with these non-essential loads are also disconnected with only the PV source module with ESS and PMA operating essential load L1-2 of 90 kW demand. Figure 8 shows the graphs of PV characteristics with respect to the changes in the system. As seen in Figure 8 the irradiation is dropped to 500 W/mt^2 creating a deficit in PV power which is compensated by the ESS module by the PMA. Figures 9(a)-9(b) show the graphs of the battery and SC characteristics responding to the changes in the PV source solar irradiation.

As observed the current discharge of the battery pack and SC increase when the solar irradiation drops at 2 sec. Figure 10 shows the voltages and power of PV ESS module and Figure 10(a) gives the graphs of the voltages at the DC link, battery, and SC maintained at 500 V, 270 V, and 300 V respectively. All the module's PV source, battery module, and SC module operate at a common DC link voltage of 500 V.

As per Figure 10(b), the power injected from 0-1 sec is 120 kW and the power is dropped to 90 kW at 2 sec when the irradiation is dropped. This compensates the local essential load of 90 kW, 10 kVAR even during grid isolation conditions with stable DC link voltage maintained by PMA. The comparative graphs Figures 11(a)-11(b) are plotted when the PMA is operated with a conventional PI controller and AF-PID controller.

Table 6. Configuration parameters

Name of the parameter	Value
Grid	100 MVA, 11 kV, 50 Hz
Feeder line	132 kV, pi section lines 50 kms each
Loads	L1-1 = 100 kW,10 kVAR; L1-2 = 90 kW, 10 kVAR; L2 = L3-1 = L3-2 = L4 = 100 kW, 50 kVAR;
DG1	PV module – 100 kW, Cin = 100uF, L1 = L2 = 1 mH, C1 = 110 uF, Cd = 12 mF.
	Battery module – Vb = 250 V, Icap =100 Ah, Lb = 5 mH, Cb = Cdb = 220 uF.
	SC module – Vsc = 300, Csc = 52F, Lsc = 5 mH, Cdsc = 220uF, Vdc ref = 500 V.
DG 2	Wind farm – PMSG - 50 kW, Rs = 0.73051 Ω, Ls = 1.2 mH, Ψ = 4.696 V.s, J = 8000 kg-mt^2, P = 15.Cin = 100 uF, Lbb = 1 mH, Cout = 1000 uF.
DG3	Fuel cell – 35 kW, Vnom = 300 V, Inom = 80 A, Vend = 125, Iend = 280 A. Cin = 100uF, Lb = 5 mH, Cd = 12mF.
ESS	Battery pack: Vbat = 250 V, 100 Ah.
	SC: C = 52 F, Rc = 8.9 mΩ, Vsc = 300 V.
	BDC: Lb = 5 mH, Cout = 220 µF,
PMA	Vdc regulator gains: Kpdc = 0.1, Kidc = 0.0023
	Current regulator gains: Kpi = 0.002, Kii = 0.00005

(a)   (b)
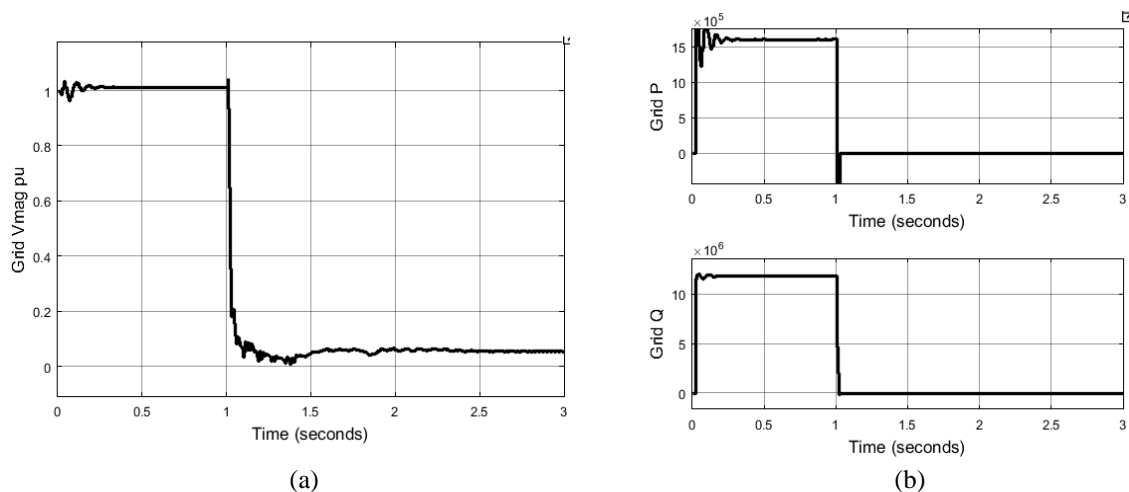
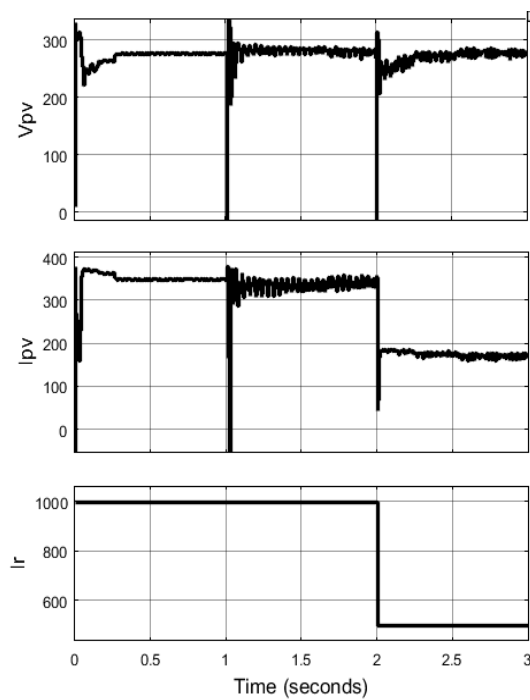Figure 7. Voltage magnitude and powers: (a) grid voltage magnitude and (b) grid active & reactive powers

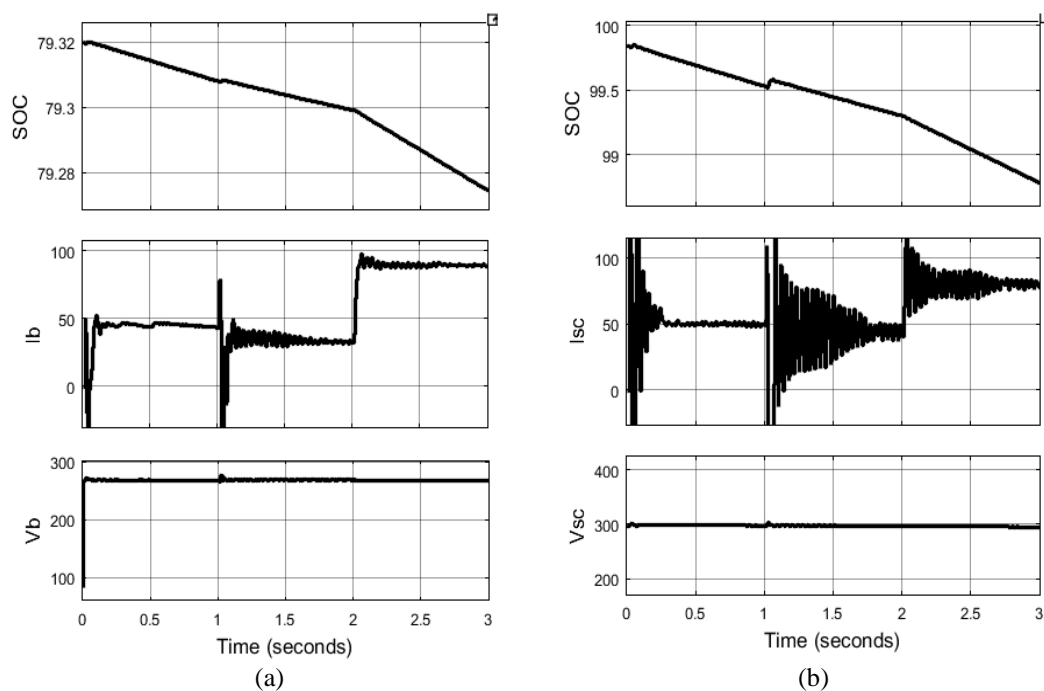Figure 8. PV array characteristics with respect to solar irradiation

(a)   (b)

Figure 9. ESS unit characteristics: (a) battery SOC, current & voltage and (b) SC SOC, current & voltage

Table 7. Comparative analysis

Name of the parameter	PI	AF-PI
Vdc peak	1340 V	750 V
Vdc ripple	10.37%	1.16%
Vdc amplitude	440 V	460 V
P injected	85 kW	90 kW

(a)   (b)
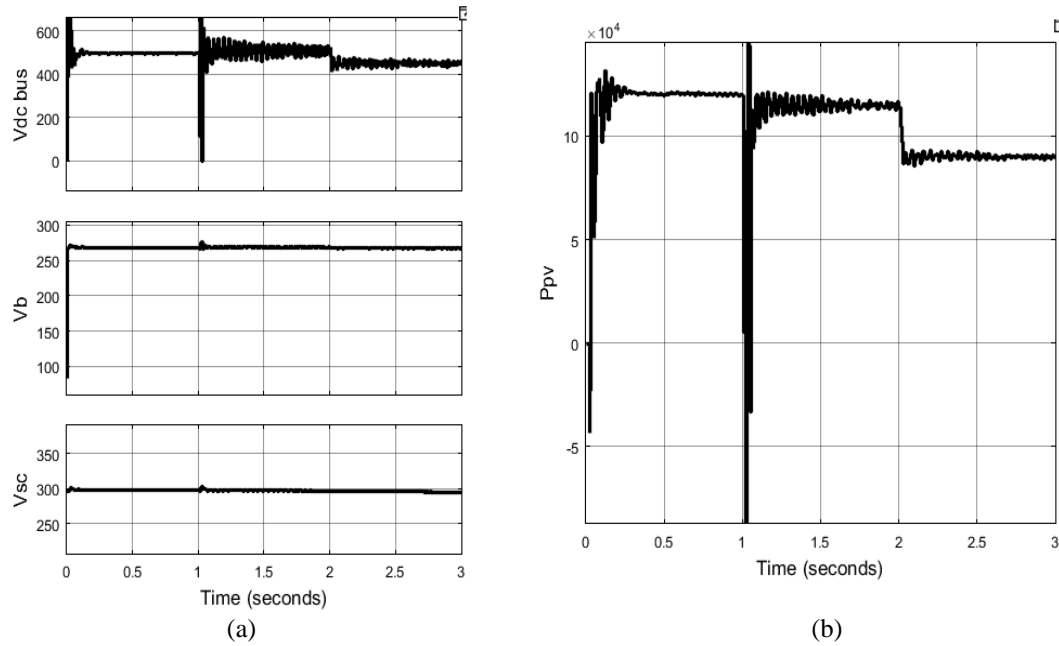
Figure 10. Voltages and power of PV ESS module: (a) voltages of DC link, battery pack, & SC and
(b) total power output of PV source module

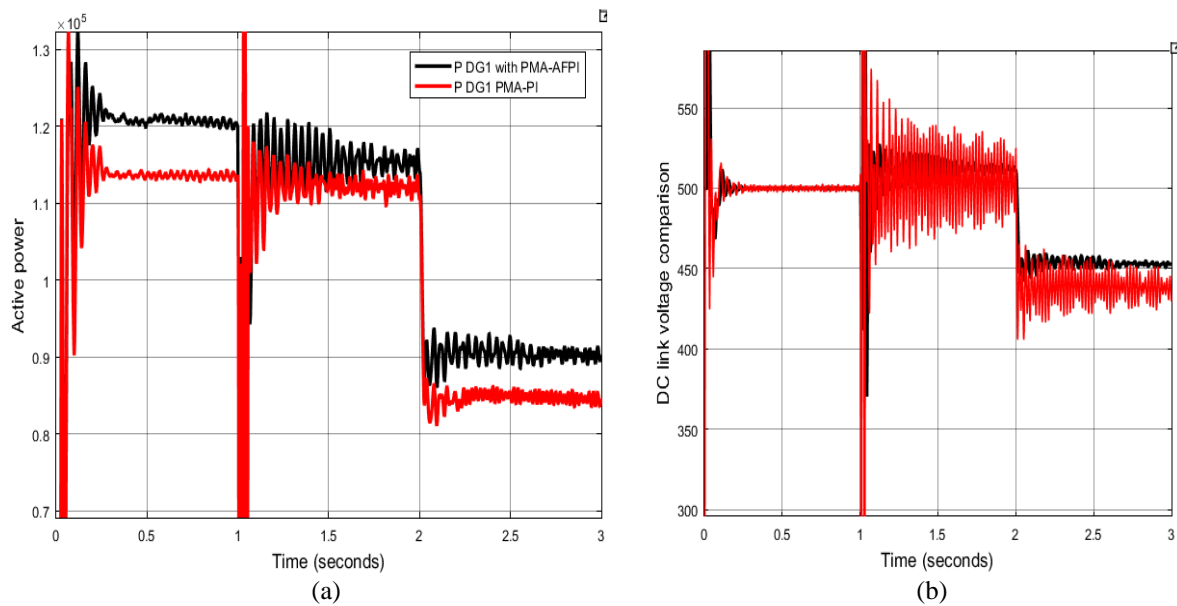(a)   (b)

Figure 11. Comparison graphs of (a) active power output of PV source module with PI & AF-PID controllers
and (b) DC link voltage of PI & AF-PID controllers

As per the given graphs, the DC link voltage is more stable and has lower peak overshoot and ripple when PMA is operated with an AF-PID controller. The injected power from the PV module is also increased as compared to PI controller. However, the voltage is maintained at 450 V which can be considered to be in limit. Figure 12 gives the graphs of the Kp1, Ki1, and Kd1 of the AF-PID controller varying with respect to changes in the grid system. A comparison table of DC link parameters and active power is given in Table 7 with conventional PI and AF-PID controllers updated in the PMA.
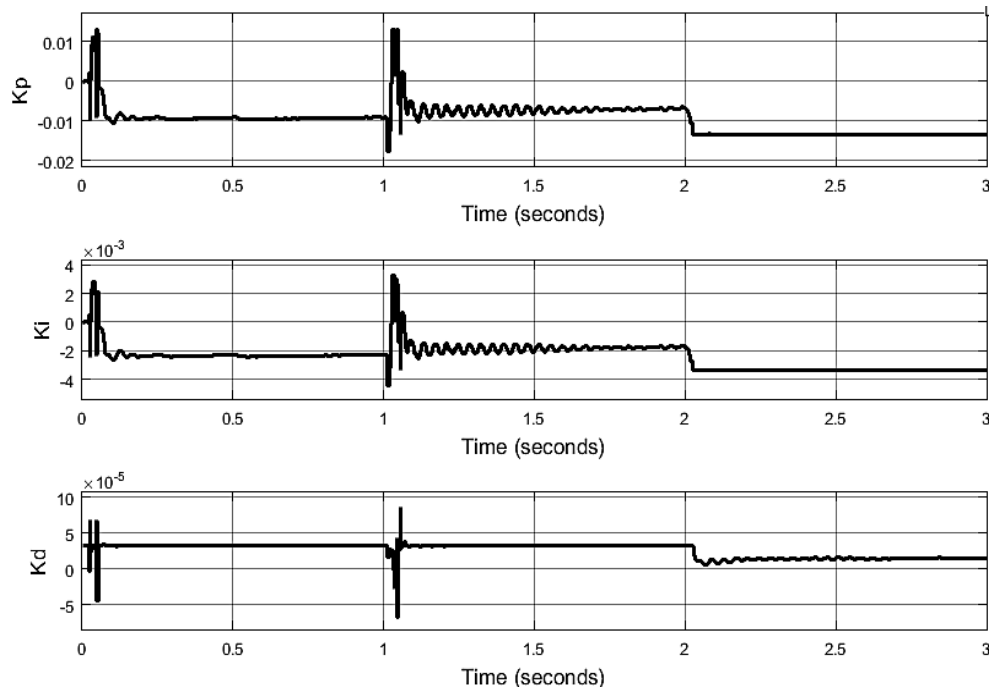
Figure 12. Dynamic Kp1, Ki1, and Kd1 gains

4. CONCLUSION

The multiple bus distribution grid is implemented with multiple loads connected to feeder line with supporting renewable sources to reduce power consumption from the main source. The update to the PV source module with ESS controlled by PMA achieves the goal of compensation of power during grid isolation condition. The PMA ensures support to the essential load during main grid source unavailability with PV source, battery and SC modules connected in parallel. The enhancement of PMA by integrating AF-PID controller replacing conventional PI controller has led to better stability of DC link voltage and more active power compensation to the load. The ripple in the DC voltage and the peak overshoot has been reduced to a great extent from 10.37% to 1.16% and 1340 V to 750 V respectively. These parametric comparisons validate the AF-PID controller is a more advanced controller with variable gain as per the given error input. During grid islanding conditions, the PI controller's gains are adjusted based on the error signal, which stabilizes the DC link voltage and active power of the PV ESS module. To further improve the performance of the PMA, the hybrid controller can be updated with optimized controller techniques that incorporate artificial intelligence, resulting in more stable voltages and power.

REFERENCES

[1]   F. Shahnia, "System of Interconnected Microgrids Challenges and Solutions." 2017, [Online]. Available: pace.ee.uwa.edu.au/wp-content/uploads/2017/03/flyer-s006.pdf.
[2]   A. Berrada and K. Loudiyi, "Optimal Modeling of Energy Storage System," *International Journal of Modeling and Optimization*, vol. 5, no. 1, pp. 71–77, 2015, doi: 10.7763/ijmo.2015.v5.439.
[3]   M. Dris and B. Djilani, "Hybrid System Power Generation'wind-photovoltaic' Connected to the Electrical Network 220 kV," *International Journal of Applied Power Engineering (IJAPE)*, vol. 7, no. 1, p. 10, Apr. 2018, doi: 10.11591/ijape.v7.i1.pp10-17.
[4]   N. Karthik, A. K. Parvathy, and R. Arul, "Optimal operation of microgrids-a survey," *International Journal of Applied Power Engineering*, vol. 7, no. 2, pp. 179–186, 2018, doi: 10.11591/ijape.v7.i2.pp181-187.
[5]   M. Katsanevakis, R. A. Stewart, and J. Lu, "Aggregated applications and benefits of energy storage systems with application-specific control methods: A review," *Renewable and Sustainable Energy Reviews*, vol. 75, pp. 719–741, 2017, doi: 10.1016/j.rser.2016.11.050.
[6]   W. Jing, C. H. Lai, W. S. H. Wong, and M. L. D. Wong, "Dynamic power allocation of battery-supercapacitor hybrid energy storage for standalone PV microgrid applications," *Sustainable Energy Technologies and Assessments*, vol. 22, pp. 55–64, 2017, doi: 10.1016/j.seta.2017.07.001.
[7]   J. Li, R. Xiong, Q. Yang, F. Liang, M. Zhang, and W. Yuan, "Design/test of a hybrid energy storage system for primary frequency control using a dynamic droop method in an isolated microgrid power system," *Applied Energy*, vol. 201, pp. 257–269, 2017, doi: 10.1016/j.apenergy.2016.10.066.
[8]   M. Faisal, M. A. Hannan, P. J. Ker, A. Hussain, M. Bin Mansor, and F. Blaabjerg, "Review of energy storage system technologies in microgrid applications: Issues and challenges," *IEEE Access*, vol. 6, pp. 35143–35164, 2018, doi: 10.1109/ACCESS.2018.2841407.

[9]   Z. Alqarni and J. A. Asumadu, "Synchronized Power Injection from PVA to Grid with Reduced THD and Dc Voltage Ripple Using PID Controller for Dc Grid Applications," in *2020 10th Annual Computing and Communication Workshop and Conference, CCWC*, 2020, pp. 248–256, doi: 10.1109/CCWC47524.2020.9031111.

[10] M. M. R. Singaravel and S. A. Daniel, "MPPT with Single DC-DC Converter and Inverter for Grid-Connected Hybrid Wind-Driven PMSG-PV System," *IEEE Transactions on Industrial Electronics*, vol. 62, no. 8, pp. 4849–4857, 2015, doi: 10.1109/TIE.2015.2399277.

[11] J. Singh and M. Ouhrouche, "MPPT Control Methods in Wind Energy Conversion Systems," *Fundamental and Advanced Topics in Wind Power*, 2011, doi: 10.5772/21657.

[12] L. Sun, G. Wu, Y. Xue, J. Shen, D. Li, and K. Y. Lee, "Coordinated control strategies for fuel cell power plant in a microgrid," *IEEE Transactions on Energy Conversion*, vol. 33, no. 1, pp. 1–9, 2018, doi: 10.1109/TEC.2017.2729881.

[13] A. Bharatee, P. K. Ray, and A. Ghosh, "A Power Management Scheme for Grid-connected PV Integrated with Hybrid Energy Storage System," *Journal of Modern Power Systems and Clean Energy*, vol. 10, no. 4, pp. 954–963, 2022, doi: 10.35833/MPCE.2021.000023.

[14] A. Bharatee, P. K. Ray, B. Subudhi, and A. Ghosh, "Power Management Strategies in a Hybrid Energy Storage System Integrated AC/DC Microgrid: A Review," *Energies*, vol. 15, no. 19, 2022, doi: 10.3390/en15197176.

[15] Z. Yi, W. Dong, and A. H. Etemadi, "A unified control and power management scheme for PV-Battery-based hybrid microgrids for both grid-connected and islanded modes," *IEEE Transactions on Smart Grid*, vol. 9, no. 6, pp. 5975–5985, 2018, doi: 10.1109/TSG.2017.2700332.

[16] N. R. Tummuru, U. Manandhar, A. Ukil, H. B. Gooi, S. K. Kollimalla, and S. Naidu, "Control strategy for AC-DC microgrid with hybrid energy storage under different operating modes," *International Journal of Electrical Power and Energy Systems*, vol. 104, pp. 807–816, 2019, doi: 10.1016/j.ijepes.2018.07.063.

[17] B. Singh, D. T. Shahani, and A. K. Verma, "IRPT based control of a 50 kw grid interfaced solar photovoltaic power generating system with power quality improvement," 2013, doi: 10.1109/PEDG.2013.6785601.

[18] N. R. Tummuru, M. K. Mishra, and S. Srinivas, "Dynamic Energy Management of Renewable Grid Integrated Hybrid Energy Storage System," *IEEE Transactions on Industrial Electronics*, vol. 62, no. 12, pp. 7728–7737, 2015, doi: 10.1109/TIE.2015.2455063.

[19] S. A. Gorji, H. G. Sahebi, M. Ektesabi, and A. B. Rad, "Topologies and control schemes of bidirectional DC–DC power converters: An overview," *IEEE Access*, vol. 7, pp. 117997–118019, 2019, doi: 10.1109/ACCESS.2019.2937239.

[20] H. Jigang, W. Jie, and F. Hui, "An anti-windup self-tuning fuzzy pid controller for speed control of brushless dc motor," *Automatika*, vol. 58, no. 3, pp. 321–335, 2017, doi: 10.1080/00051144.2018.1423724.

[21] A. Badie Sharkawy, "Genetic fuzzy self-tuning PID controllers for antilock braking systems," *Engineering Applications of Artificial Intelligence*, vol. 23, no. 7, pp. 1041–1052, 2010, doi: 10.1016/j.engappai.2010.06.011.

[22] H. Wang, F. Zhang, P. Liu, and G. Li, "Test system design of lithium battery based on fuzzy self-tuning PID control," in *Proceedings - 8th International Conference on Future Generation Communication and Networking, FGCN 2014*, 2014, pp. 96–99, doi: 10.1109/FGCN.2014.31.

[23] K. F. Hussein, I. Abdel-Qader, and M. K. Hussain, "Hybrid fuzzy PID controller for buck-boost converter in solar energy-battery systems," *IEEE International Conference on Electro Information Technology*, vol. 2015-June, pp. 70–75, 2015, doi: 10.1109/EIT.2015.7293323.

[24] S. Y. Vamsi Kumar, M. Mukku, V. K. Jonnalagadda, A. Gudidh, and P. Kumar, "Speed Control Analysis of an Electrical Vehicle by Using Fuzzy- PID and ANFIS Controllers," 2022, doi: 10.1109/C2I456876.2022.10051235.

[25] S. Kotra and M. K. Mishra, "A supervisory power management system for a hybrid microgrid with HESS," *IEEE Transactions on Industrial Electronics*, vol. 64, no. 5, pp. 3640–3649, 2017, doi: 10.1109/TIE.2017.2652345.

BIOGRAPHIES OF AUTHORS

Veeranjaneyulu Gopu is received the B.Tech. degree from the Department of Electrical and Electronics Engineering, Jawaharlal Nehru Technological University, Hyderabad, in 2007, and M.Tech. degree from Power Systems Engineering, Acharya Nagarjuna University, Guntur, in 2009. He is currently pursuing a Ph.D. degree at Visvesvaraya Technological University, Belagavi. He has been an assistant professor at RVR&JC College of Engineering, Guntur, India since 2013. His research interests include the field of power systems, power electronics, motor drives, renewable energy, and microgrids. He can be contacted at email: gvanjaneyulu@rvrjc.ac.in or gvvtu2023@mail.com.

Mudakapla Shadaksharappa Nagaraj is presently working as a professor and head in the Department of Electrical and Electronic Engineering, BIET, Davangere since 2008. He completed his B.E. (E & E) degree from Government BDT College of Engineering, Davangere, Mysore University in 1986 and received his master's degree in Power Systems from NIE, Mysore, Mysore University in 1990. He received his doctorate from Visvesvaraya Technological University in 2008. Presently, he is guiding 2 Ph.D. students and 5 research scholars are awarded with Ph.D. under VTU, Belagavi. His research interests include the fields of electrical load forecasting, reactive power compensation, economic scheduling, contingency analysis, control systems, power electronics, artificial neural networks, and fuzzy logic. He has published more than 40 papers in these areas in refereed international/national journals and conference proceedings. He is life member of the Indian Society for Technical Education and a Member of the Institution of Engineers (MIE). He can be contacted at email: msndvg@gmail.com.